ELSEVIER

Journal of Nuclear Materials 246 (1997) 9–16

journal of nuclear materials

Quantitative AMS depth profiling of the hydrogen isotopes collected in graphite divertor and wall tiles of the tokamak ASDEX-Upgrade

G.Y. Sun [a], M. Friedrich [a], R. Grötzschel [a], W. Bürger [a], R. Behrisch [b,*], C. García-Rosales [b,1]

[a] *Forschungszentrum Rossendorf, PO Box 510119, D-01314 Dresden, Germany*
[b] *Max-Planck-Institut für Plasmaphysik, Euratom association, D-85748 Garching, Germany*

Received 20 November 1996; accepted 4 April 1997

Abstract

The accelerator mass spectrometry (AMS) facility at the 3 MV Tandetron in Rossendorf has been applied for quantitative depth profiling of deuterium and tritium in samples cut from graphite protection tiles at the vessel walls of the fusion experiment ASDEX-Upgrade at the Max-Planck-Institut für Plasmaphysik in Garching. The tritium originates from D(d,p)T fusion reactions in the plasma and it is implanted in the vessel walls together with deuterium atoms and ions from the plasma. The T concentrations in the surface layers down to the analyzing depth of about 25 μm are in the range of 10^{11} to 5×10^{15} T-atoms/cm^3 corresponding to a tritium retention of 3×10^{10} to 3.5×10^{12} T-atoms/cm^2. The much higher deuterium concentrations in the samples were simultaneously measured by calibrated conventional SIMS. In the surface layers down to the analyzing depth of about 25 μm the deuterium concentrations are between 3×10^{18} and 8×10^{21} atoms/cm^3, corresponding to a deuterium retention of 2.5×10^{16} to 2.5×10^{18} atoms/cm^2 The estimated total amount of tritium in the vessel walls is of the same order of magnitude as the total number of neutrons produced in D(d,n)^{3}He reactions. © 1997 Elsevier Science B.V.

1. Introduction

Implantation, codeposition, retention, and release of hydrogen isotopes in the surface layers of the plasma facing material at the vessel walls of fusion devices plays an important role in fusion research with respect to wall pumping and recycling of the hydrogen isotopes from the vessel walls. These processes largely contribute to the plasma density and isotope composition [1–7]. Further, for a D, T fusion plasma, the tritium trapped in the plasma-facing areas of the vessel walls represents a very critical radioactive inventory [8]. One means to get some understanding for a possible control of these processes are detailed measurements of the concentration and depth profiles of the hydrogen isotopes which build up in today's fusion experiments at different first wall areas. For quantitative depth profiling of hydrogen isotopes in the surface layers of solids several methods can be applied [9,10], such as: nuclear reaction analysis (NRA) [10–12], elastic proton backscattering [13], elastic recoil detection analysis (ERDA) [14–18], and secondary ion mass spectrometry (SIMS) [19–21]. For the detection of the very small amounts of tritium, such as those deposited in the vessel walls of today's fusion experiments with a deuterium plasma [22–24], the sensitivities of the first three techniques are generally not sufficient, while in conventional SIMS the interference with the molecular ions HD and H_3 cannot be suppressed sufficiently. Measurements based on the tritium decay using Pin diodes [22] or conventional scintillation counters [23,24] are sensitive only to the very surface layers and require special sample preparation [23].

One of the most sensitive methods for analyzing low

* Corresponding author. Tel.: +49-89 3299 1250; fax: +49-89 3299 1149; E-mail: reb@ipp.mpg.de.

[1] Permanent address: Centro de Estudios e Investigaciones Técnicas de Guipuzcoa (CEIT), POB 1555, 20080 San Sebastian, Spain.

PII S0022-3115(97)00080-9

concentrations of isotopes is accelerator mass spectrometry (AMS) [25–27]. In recent years it has been developed to a standard method for the measurement of concentration depth profiles of trace elements [28–30] in solids. This method represents basically an extension of a negative secondary ion mass spectrometer with a magnetic mass separator of low mass resolution, but large acceptance angle. Additionally to the conventional Faraday cup or channeltron detector for measuring the secondary ion intensity, a special detection system consisting of an MeV tandem accelerator and a subsequent nuclear spectrometry system is used. The sputtered negative secondary ions of a selected mass are injected into the first stage of the accelerator and are accelerated to a few MeV. At the positive high voltage terminal the ions pass through a gas or foil stripper, where nearly all molecules disintegrate to atoms which get positively charged with a charge state distribution depending on ion species and energy and on the stripper parameters [31]. These singly or multiply charged positive ions are further accelerated in the second stage of the tandem to a final energy according to their charge state. The MeV ions are subsequently detected by means of a combination of electrostatic and magnetic fields and a nuclear particle detector being able to analyze energy, mass and/or atomic number Z of the ions. Thus the atomic ions can be further separated from the very few molecular ions which were not disintegrated in the stripper and may reach the detector. Suppression factors for molecular ions of more than 10^{13} are achievable by AMS.

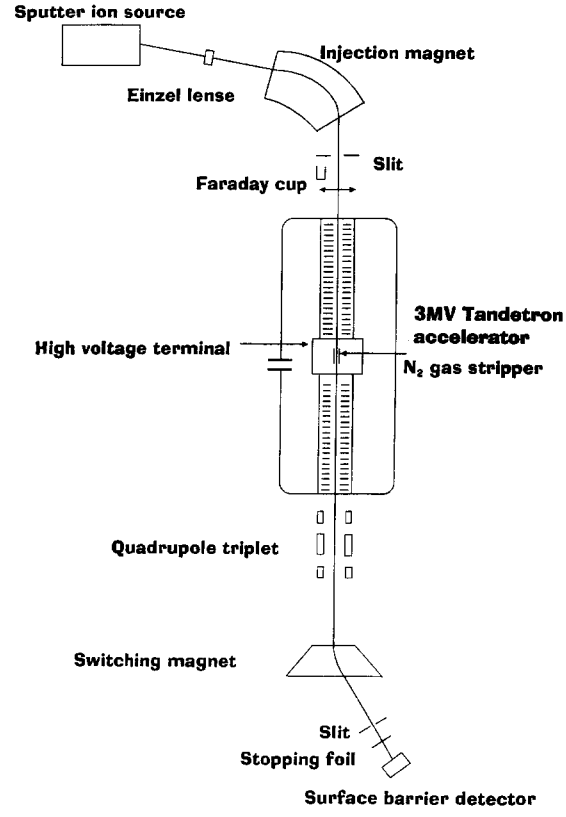

Fig. 1. Schematic diagram of the accelerator mass spectrometer (AMS) set-up.

2. Experimental

At the Rossendorf 3 MV Tandetron accelerator [30] an AMS facility has been installed especially for analysis of hydrogen isotopes and employed for the depth profiling of these isotopes in plasma exposed graphite materials of the tokamak ASDEX-Upgrade [32,33]. Fig. 1 shows schematically the main components of the AMS set-up.The sample to be analyzed is inserted into the standard IONEX 860-C caesium sputter ion source using a modified target rod. The sputtered negative ions are extracted from the sample by a voltage of 23 kV and focused with an einzel lens. They are mass analyzed by means of the wide-gap double-focusing 80° injection magnet providing a large acceptance angle and, using an exit aperture of 4×6 mm^2, a mass resolution $M/\Delta M$ of about 100 [34], which is sufficient for the interesting low mass constituents of the investigated material. Just behind the exit aperture near the entrance of the accelerator a retractable Faraday cup is used for the measurement of the high intensity ion components, such as D and ^{12}C in these measurements. If just this ion current is measured we talk in the following of 'conventional SIMS mode'. For switching to the different masses the magnet was controlled by a Hall probe. The D^- signal in these conventional SIMS measurements can be falsified by the presence of H_2^- ions. Both are present because the hydrogen and deuterium concentrations in the samples are expected to be similar [17,35,36]. However, the formation probability of H_2^- ions in the Cs^+ sputter ion source is low, the ratio of H_2^-/H^- being about 10^{-5} [26], i.e., the contribution of H_2^- ions to the D^- ion signal is small and can be neglected.

For the tritium depth profiling the negative ions with mass $M = 3$, i.e., T^-, HD^-, H_3^- ions are selected by the injection magnet. They are injected and accelerated in the Tandetron to the positive terminal voltage of 1.5 MV where they are stripped and split up in the N_2 gas cell and subsequently accelerated back to ground potential. They are again mass analyzed in the switching magnet set for three MeV ions with mass $M = 3$. For counting the tritium ions and separating them from molecular ions we used an implanted silicon surface barrier detector covered with a 17 μm thick Al foil. The few HD^+ ions in the beam were cracked in the foil to 1 MeV protons and 2 MeV deuterons. The 1 MeV protons having a mean projected range of 14.3 μm are fully stopped in the Al foil, while the 2 MeV deuterons leave the foil with a residual energy of about 1.1 MeV. They can be separated in the detector from T^+-ions which have a residual energy of about 2.1 MeV after

passing the foil. In the deuterium plasma of the fusion experiment ASDEX-Upgrade also ^{3}He-ions are produced by the D(d,p)^{3}He reaction and they are also implanted into the vessel walls. However, in sputter ion sources the formation of negative He ions is very unlikely and 3 MeV He ions would be lost in the stopping foil, so that any interference with tritium can be excluded.

In order to obtain the real depth profile, the crater formed by sputtering should have a flat bottom and ions sputtered from the side walls of the crater should not be detected [20,21]. The usual way of scanning the primary sputtering beam across the surface in order to achieve uniform erosion is not possible with the ion source used here. Therefore in our case the sample was scanned mechanically by two off-axis disks which were driven by two synchronous motors with different frequencies [30], allowing to scan the sample in an area of a parallelogram of about 2.5×2.5 mm^2 (Fig. 2) under the stationary beam. Furthermore a copper diaphragm with a 1.5 mm circular opening was used in front of the sample [30] and a negative voltage was applied to the target holder. The small opening acts like an immersion lens [39] which focuses the secondary ions so that the ions generated at the side wall of the crater could not pass through the aperture of the ionizer. Finally an electronic gating is used to collect the signals only when the sputtering ion beam hits the center of the crater, i.e., only about 10% of the rastered area is analyzed (Fig. 2). Due to the relatively large diameter of the Cs^+-ion beam (FWHM is about 200 μm) the tail of the Cs beam may reach the side wall region even during the gating time. The formation of a crater wall could be avoided by cutting a groove in the sample surface at the area where the crater wall develops [30]. The improvement obtained with these provisions is demonstrated in Fig. 3, showing the deuterium-depth profile measured in SIMS mode for a graphite EK98 calibration sample, which had been implanted with 210 keV deuterium to a fluence of 10^{16} cm^{-2}. With electronic gating and sample shaping the contribution from the side wall, which distorts the depth profile and pretends a tail to a larger depth, is suppressed. After each analysis the depth of the sputtered crater was profiled with a Dektak 8000 [30]. The depth scale was calibrated assuming a constant sputtering yield independent on the hydrogen concentration.

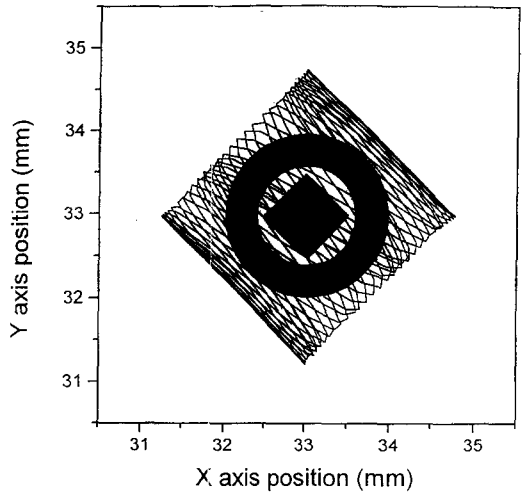

Fig. 2. Cs^+ ion impact lines on the wobbled sample. The central marked part indicates the area of data collection, the marked ring indicates the groove.

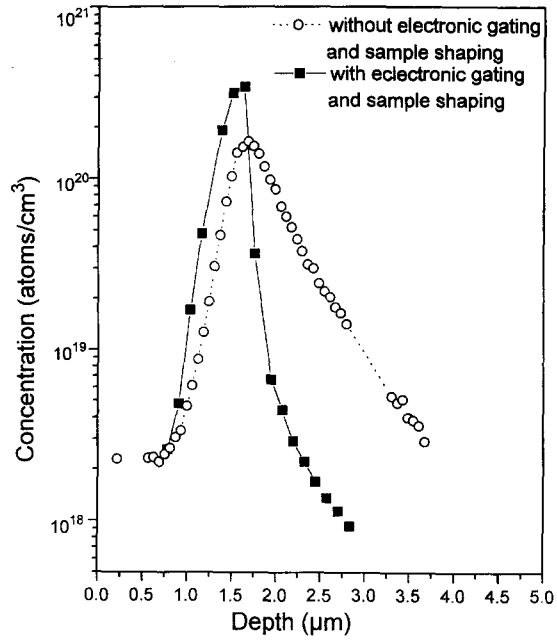

Fig. 3. Depth profiles of deuterium which had been implanted in Graphite EK98 with an energy of 210 keV at a fluence of 1×10^{16} D/cm^2.

3. Evaluation of the AMS and SIMS measurements

In the SIMS mode the secondary ion intensity or count rate N_i for an isotope of species 'i' is given by

$$N_i = I_s Y_i f_i T_i C_i, \quad (1)$$

where I_s is the primary sputter beam current, Y_i the sputtering yield for this isotope, f_i the fraction of sputtered atoms released as negative ions, C_i the isotopic concentration in the sample and the term T_i represents the detection efficiency, mainly determined by ion extraction geometry and acceptance angle of the detection system. Thus the observed count rate N_i is correlated with the concentration C_i by

$$C_i = N_i/(I_s Y_i f_i T_i) \quad \text{or} \quad C_i = N_i/(I_s S_i). \quad (2)$$

The factor $S_i = Y_i f_i T_i$ differs for different ions and is difficult to be determined by experiments. For a quantitative analysis therefore a second sputtered ion species 'm' representing the matrix is measured simultaneously. The measured relative yields are then given by

$$N_i/N_m = C_i S_i/(C_m S_m) \quad (3)$$

and we get the relative concentration

$$C_i/C_m = (N_i/N_m) S_m/S_i. \quad (4)$$

For the analysis of a small impurity concentration C_i in a constant matrix a 'relative sensitivity factor'(RSF) was introduced in SIMS [20] as a conversion factor from secondary ion intensity to atom concentration:

$$C_i = (N_i/N_m)\mathrm{RSF}, \quad (5)$$

where $\mathrm{RSF} = (S_m/S_i)C_m$ has the dimension of an atomic concentration.

In the case of AMS additional calibration terms must be included for the specific probability of electron loss in the stripper to the selected positive charge state, the transmission losses in the accelerator and the beam line components, and the detector efficiency. The efficiency of the nuclear particle detectors is mostly close to unity and the other parameters may be expressed for each ion species by a single term P_i being the ratio between the number of positive ions measured by the detector to the number of negative ions entering the accelerator. The measured AMS yield $N_{i,\mathrm{AMS}}$ is then expressed as

$$N_{i,\mathrm{AMS}} = N_i P_i \quad (6)$$

and the impurity concentration C_i can be calculated with Eq. (5) to be

$$C_i = N_{i,\mathrm{AMS}}/(P_i N_m)\mathrm{RSF}. \quad (7)$$

The parameter P_i depends strongly on the gas pressure in the stripper and on the ion optical properties of the accelerator and must be measured for each ion species individually. In this work we measured the RSF for D in C using the graphite EK 98 calibration sample, which had been implanted with a fluence of 10^{16} D/cm^2 at an energy of 210 keV, and determined a value of $\mathrm{RSF}_{D/C} = 3.2 \times 10^{23}$ atoms/cm^3. Due to the lack of an equivalent implanted tritium calibration sample it is assumed that the RSF values for deuterium and tritium in graphite are about equal.

The tritium content in the ASDEX Upgrade samples is so low that they cannot be used to determine the accelerator transmission factor P_T for tritium. For determining P_T a tritium enriched titanium hydride sample with a known T/H atomic concentration ratio of 3.0×10^{-10} (obtained from Lawrence Livermore National Laboratory, USA) was used. The H^--ion intensity N_H was measured in the SIMS mode and simultaneously the tritium ion intensity $N_{T,\mathrm{AMS}}$ in the AMS mode. Then we get

$$P_T = (N_{T,\mathrm{AMS}}/N_{H,\mathrm{SIMS}})(C_H/C_T). \quad (8)$$

Here we have to assume the same RSF or the same ratios S_m/S_i for H and T, i.e., the differences in the sputtering yields, the probabilities for forming negative hydrogen ions in the Cs sputter ion source and the detection probabilities are assumed to be negligible. There are no experimental data available, however data obtained for other systems [35] indicate that the probabilities for forming negative hydrogen ions depend on the sputtered atom velocity. Consequently S_T may be smaller than S_H by $(M_T/M_H)^{1/2} = 1.73$ for H and T sputtered with the same energy. By assuming S_T and S_H to be equal the tritium concentrations may be underestimated by up to this factor. This is the major uncertainty in the calibrations, resulting in a maximum possible error in the measurements below a factor of two.

Finally, the background in the tritium count rate analyzing a new EK 98 graphite target was measured to be about 20 counts/s mainly due to a memory effect of the ion source which could not yet been clearly identified. Accordingly, our detection limit for tritium in graphite is about 10^{11} atoms/cm^3, being much lower than the concentrations measured here. For deuterium in graphite our detection limit is about 10^{18} atoms/cm^3, which is given by the residual water vapor in the ion source. A higher sensitivity could be obtained for the hydrogen isotopes if the background can be reduced, such as by the use of a very clean ion source, ultra-high vacuum in the system and an externally mass analyzed Cs ion beam for sputtering [29].

4. Samples from the vessel walls of ASDEX-Upgrade

ASDEX-Upgrade is a fusion experiment of the Tokamak type with an axissymmetric divertor (axis symmetric divertor experiment) [32,33]. The plasma is produced by an induced electrical current in a toroidal discharge chamber with a major radius of about 1.65 m, a horizontal minor radius of 0.5 m, and an elongation of 1.6. The plasma volume is about 12 m^3, and the area of the plasma-facing surface is about 70 m^2. A major part of the plasma facing areas has been covered by tiles of fine grain graphite EK 98. Out of this, the areas of the lower inner and outer divertors tiles are about 3.5 m^2 and 4.5 m^2, respectively. At the inner wall the fine grain graphite protection tiles have an area of about 8.5 m^2, and on the passive stabilizing loops they have an area of about 5 m^2 each (Fig. 4).

Before installation in 1991 the graphite tiles have been degassed in vacuum for about two hours at temperatures of 1800 K to 2100 K. Further, before each experimental tokamak discharge campaign the vessel had been heated to 420 K for about one week. After baking, the inner parts of the vessel were boronized by running a glow discharge in diborane and He. Surface layer analysis showed that the total amount of B deposited on the vessel walls was about 3×10^{16} to 2×10^{17} B/cm^2. Further, during the last two

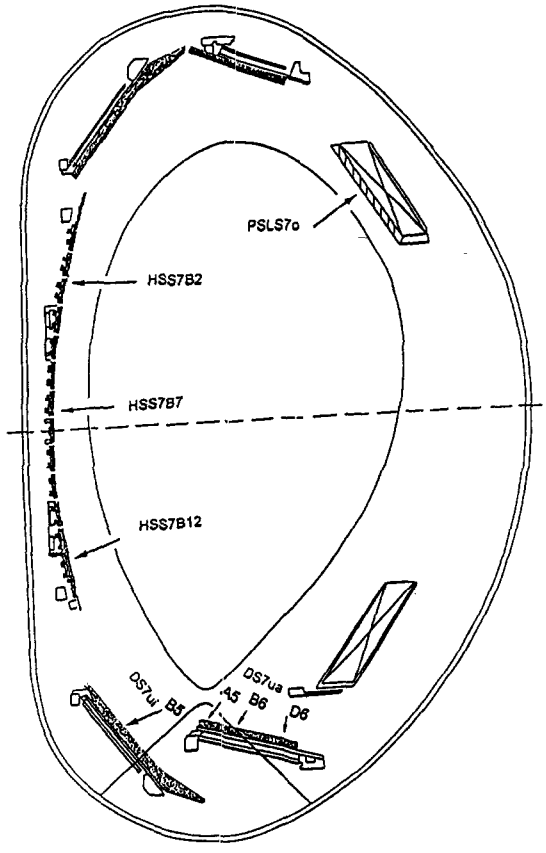

Fig. 4. Cut through the vessel of the divertor tokamak fusion experiment ASDEX-upgrade showing the positions of the samples which have been analyzed.

discharge periods in 1993/94, and 1994/95 glow discharges in He have been applied between the tokamak discharges [38].

The graphite tiles have been subjected to four experimental tokamak discharge campaigns, each lasting for about one year. There have been about 1800 'Ohmic discharges' with a toroidal magnetic field in the range of $1\text{T} \leq B_t \leq 3\text{T}$ and flat-top plasma currents between 0.3 MA and 1.2 MA, each lasting about 4 s resulting in a total discharge time of about 2 h. The gas filling was mostly deuterium and line average plasma densities were about $n_e \cong 6\text{–}8 \times 10^{19}/\text{m}^3$. Out of these in about 440 discharges of the 1993/94 and 1994/95 experimental periods the plasma was additionally heated by injecting neutral beams of deuterium at an acceleration voltage of 63 keV resulting in a heating power ≤ 10 MW lasting for about 2 s. About 240 discharges were additionally heated by injecting neutral beams of hydrogen at an acceleration voltage of 55 keV resulting in a heating power ≤ 7 MW and lasting for about 2 s. Finally about 220 discharges were additionally heated by ion cyclotron resonance heating (ICRH) with a frequency in the range between 30 and 120 MHz, and a maximum power of 3 MW. The maximum plasma temperature was in the keV range, the maximum power density on the outer divertor tiles was about 5–6 MW/m^2, resulting in a peak temperature of the graphite divertor tiles below 600 K [38].

In the D, D discharges, especially those with additional heating, some D, D fusion reactions take place. They have two equally probable branches,

$$\text{D} + \text{D} \rightarrow {}^3\text{He}\ (0.82\ \text{MeV}) + \text{n}\ (2.45\,\text{MeV}),$$

$$\text{D} + \text{D} \rightarrow \text{T}\ (1.01\ \text{MeV}) + \text{H}\ (3.02\ \text{MeV}).$$

During the discharge period when the wall tiles had been installed about 3×10^{17} neutrons had been produced in total [40]. This gives also the total number of T atoms produced in the plasma

Out of the 1 MeV tritium ions which are predominantly generated in the center of the plasma generally about 2/3 are confined and thermalized in the plasma during the discharge. About 1/3 of the tritium leaves the plasma immediately on drift orbits with only minor slowing down in the plasma. Most of them impinge onto the vessel walls with nearly their full energy and a broad distribution in angles of incidence and they are implanted into the surface layers of the vessel walls. The vessel walls are also implanted with low energy tritium ions and with low energy deuterium ions and neutrals from the plasma, as well as with the ^{3}He (0.8 MeV) from the fusion reactions. Finally they are bombarded with impurity ions from the plasma, such as graphite predominantly at energies in the 100 eV range and at some areas, such as the inner divertor, Carbon built-up was found. Due to the still relatively few D, D reactions in the plasma the concentrations of deuterium which are built up in the graphite wall tiles are much higher than those of tritium, while ^{3}He is not well trapped in graphite. Assuming toroidally and poloidally uniform implantation of the produced T into the vessel walls a mean amount of retained T of about 4.5×10^{11} T/cm^2 can be expected, well above the detection limit of these AMS measurements.

After the 1994/95 discharge period small samples have been cut from several representative areas of the fine grain graphite tiles and they have been analyzed in Rossendorf for the T- and D-depth profiles. Further samples cut from the tiles have been analyzed by quantitative temperature controlled desorption (TCD) [37,38].

5. Results

With the calibrated AMS and SIMS facility the tritium depth profiles were measured simultaneously with the deuterium profiles for the following plasma facing graphite samples of sector 7 (S7) removed from the fusion experiment ASDEX-Upgrade (see Fig. 4): outer lower divertor tiles (DS7 ua.) A5, B6, D6; inner lower divertor tiles (DS7

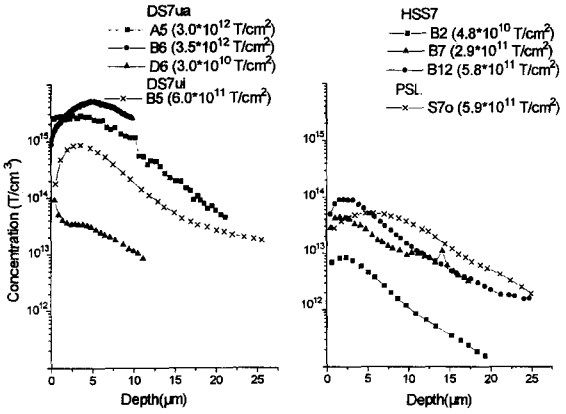

Fig. 5. Depth profiles of tritium in the divertor and in protection limiters.

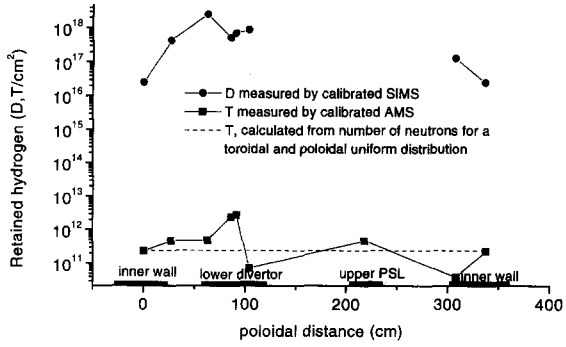

Fig. 7. Poloidal distribution of tritium and deuterium in the surface layers of tiles from the ASDEX-upgrade divertor tokamak fusion experiment.

ui.) B5; inner wall tiles: (HSS7) B2, B7, and B12; and tiles from the graphite protection plate on the upper passive Cu-stabilization loop (PSL S7o).

The measured tritium and deuterium depth profiles are shown in Figs. 5 and 6. The amounts of D and T trapped per unit area, which are obtained by integrating the depth distributions down to the measured depth are also given in the figures. Due to the measured finite depth they represent lower limits for the T and D inventories. The deuterium concentrations peak close to the surface with values of up to 10^{22} D/cm^3 at the divertor plates and 2×10^{21} D/cm^3 at the inner wall tiles. The tritium concentrations have a broad maximum at depths of about 5 μm at the divertor tiles and at about 2 to 3 μm at the inner wall and protection tiles. The tritium concentrations are about a factor of 10^6 lower than the deuterium concentrations and reach values of 5×10^{15} T/cm^3 at the divertor plates and about 10^{14} T/cm^3 at the inner wall- and protection tiles. The depth profiles of both, the tritium and deuterium were found to exceed the measuring depth of about 25 μm.

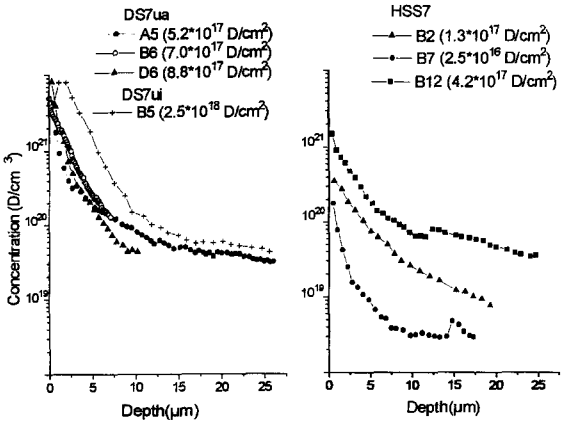

Fig. 6. Depth profiles of deuterium in the divertor and in protection limiters.

The measured areal density of deposited tritium and deuterium is plotted in dependence of the poloidal position in Fig. 7. The results show that the tritium concentration in the lower divertor plates is more than an order of magnitude higher than on the other areas. This is expected from the configuration of the confining magnetic field where the $\nabla B \times B$ force causes a dominant drift to the lower divertor plates. The low concentration at one edge of the inner divertor tile (sample B6) is due to shadowing of the magnetic field lines by the outer divertor plate. The horizontal dashed line in Fig. 7 shows the calculated tritium concentrations as expected from the total amount of produced neutrons [40] for a uniform distribution of the tritium on the vessel walls.

6. Discussion

The measured ratio of T/D being about 10^{-6} in the wall samples reflects the very low D(d,n)T fusion- and tritium production rate in the plasma. While a fraction of the tritium is implanted into the vessel walls with energies of up to 1 MeV, the rest of the tritium and the deuterium from the plasma impinges onto the vessel walls with much lower energies, i.e., in the 100 eV range, except for a low flux of energetic neutral deuterium and tritium atoms with energies up to the keV range which are produced in the plasma by charge exchange collisions [41]. The mean projected range of 1 MeV tritium at normal incidence in graphite is about (8.5 ± 0.05) μm, while the mean range of 100 eV to 1 keV deuterium ions is $< 0.015 \pm 0.01$ μm [42]. The broad peak in the ranges for tritium at about 5 to 8 μm likely reflects the large impact energy of some of the tritium.

However, the measured depth distributions of tritium and deuterium ranging to ≥ 25 μm are not expected from the known ion ranges, they exceed the mean projected

ranges for implantation at normal incidence [42]. The measured range distributions may be explained by the following processes:

– The tritium impinges onto the vessel walls with a broad angular and energy distribution resulting in a shift of the peak in the range toward the surface.

– During a plasma discharge also graphite originating predominantly from erosion dominated areas, such as the inner wall graphite protection shield, is redeposited onto the divertor plates and other areas of the vessel walls together with the implantation of tritium and deuterium. At such deposition dominated areas layers saturated with the discharge gas have been found to build up [43], due to co-deposition or co-implantation [44]. At a divertor with a low plasma temperature, such as in ASDEX-upgrade [46], the co-deposition may cause the build-up of thicker layers especially at the areas outside the strike area of the separatrix.

– Diffusion of the implanted hydrogen occurs deep into the sample beyond the range of implantation.

– Finally the analyzed surfaces are rough in the μm range. This may cause errors in the depth distribution measurements.

– The baking of the vessel walls to 420 K after each opening of the vessel is not expected to cause hydrogen isotope release [38]. The B deposited during boronisation is too small to influence the T retention. However the glow discharges in He may contribute to release T from surface layers with a depth of the order of ≤ 0.1 μm. Some T may further be released by isotope exchange during venting of the vessel.

The measured amount of tritium retained per unit area within the measured depth of about 25 μm is mostly lower, and at some areas, such as on the divertor plates, also higher than corresponding to a uniform distribution of the produced tritium on the vessel walls (Fig. 7). Taking into account the uncertainties in the neutron measurements and the calibration for the tritium measurements, and that tritium was measured only at a few positions, it is not possible to extrapolate to the total amount of tritium collected in the vessel walls. The amount of T measured at the few areas of the vessel walls indicates, however, that a major fraction of the produced tritium may be retained in the vessel walls.

The maximum local hydrogen concentrations in the wall tiles obtained by adding the deuterium and tritium amounts, giving 5×10^{19} to 8×10^{21} $(D + T)/cm^3$ are still below the expected saturation concentration for the hydrogen isotopes at implantation in graphite being about $3 \times 10^{22}/cm^3$ [45]. This is in agreement with other measurements of the retained H and D by ERDA and temperature controlled desorption (TCD) of the plasma-facing graphite tiles. In these investigations hydrogen concentrations larger than the D concentrations with $H/D \simeq 3$ to 4 have been found [38].

7. Conclusions

AMS depth profiling has been successfully applied for depth profiling of tritium in graphite samples from the fusion experiment ASDEX-Upgrade. A depth range larger than 25 μm can be analyzed. A distortion of the depth profile in the measurements due to edge effects at the sputtered area can be prevented by electronic gating and sample shaping. Instead of scanning the Cs beam, wobbling of the sample has been successfully used for sensitive sputter depth profiling. The tritium is found in graphite samples from the vessel walls at depths > 25 μm, which is much larger than the mean projected range for implantation of the 1 MeV tritium ions, as produced in the plasma. Deuterium from the plasma which impinges onto the vessel walls at much lower energies has been measured up to the similar depth. This may be due to the implantation of deuterium and tritium together with deposition of graphite (codeposition) which is eroded by chemical sputtering from the inner wall graphite protection plates. The large depth may also be due to diffusion of the implanted tritium and deuterium into the bulk of the graphite.

The measured (D + T) concentrations in the graphite tiles from the vessel walls are generally below the expected saturation concentration of hydrogen isotopes at implantation in graphite, in agreement with the presence of larger concentrations of hydrogen in the vessel walls, as found by other investigations. The tritium is not uniformly distributed on the different areas of the vessel wall. The highest concentration is found at the inner divertor plates at the area where the separatrix intersects. The measured neutron fluence is of the order of the amount of tritium produced by D(d,p)T fusion reactions in the plasma.

Acknowledgements

The authors wish to thank Mrs R. Aniol for surface profile measurements and the staff of the Rossendorf accelerator department for construction of the beam line, sample preparation and ion source modification. G.Y.S. would like to thank Mr F. Herman and Mr K. Brankoff for the valuable discussions on compiling the data acquisition program. We would also like to thank S. Bosch, P. Franzen and W. Möller for critical reading of the manuscript and many helpful comments. This work is supported by Bundesministerium für Bildung, Wissenschaft, Forschung und Technologie, project BMFT KKS 06 DR 666 I/TP:8.

References

[1] G.M. McCracken, S.J. Fielding, S.K. Ehrents, A. Pospieczyk, P.E. Stott, Nucl. Fus. 18 (1978) 35.
[2] TFR Group, J. Nucl. Mater. 76&77 (1978) 578.

[3] G.M. McCracken, P. Stott, Nucl. Fusion 19 (1979) 889.
[4] TFR Group, presented by P. Platz, J. Nucl. Mater. 93&94 (1980) 173.
[5] R. Behrisch, 'Physics of plasmas close to thermonuclear conditions', in: Proc. of a course held in Varenna, Italy, 27 Aug.–8 Sept. 1979, ed. B. Coppi, G.G. Leotta, D. Pfirsch, R. Pozzoli and E. Sindoni, Vol. I (1980) p. 425, Commission of the European communities, EUR FU BRU/XII/476/80.
[6] J. Ehrenberg, in: Physical Processes of the Interaction of Fusion Plasmas with Solids, ed. W.O. Hofer and J. Roth (Academic Press, New York, 1996) p. 38.
[7] P. Andrew, M. Pick, J. Nucl. Mater. 220–222 (1995) 601.
[8] G. Federici, R. Causey, P.L. Andrew, C.H. Wu, Fusion Eng. Design 28 (1995) 1356.
[9] J.F. Ziegler, C.P. Wu, P. Williams, C.W. White, B. Terreault, B.M.U. Scherzer, R.L. Schulte, E.J. Schneid, C.W. Magee, E. Ligeon, J. L'Ecuyere, W.A. Lanford, F.J. Kuehne, E.A. Kamykowski, W.O. Hofer, A. Guivarche, C.H. Filleix, V.R. Deline, C.A. Evans Jr., B.L. Cohen, G.J. Clark, W.K. Chu, C. Brassard, R.S. Blewer, R. Behrisch, B.R. Appleton, D.D. Allred, Nucl. Instrum. Methods 149 (1978) 19.
[10] J. Bøttiger, J. Nucl. Mater. 78 (1978) 161.
[11] C.J. Altstetter, R. Behrisch, J. Bøttiger, F. Pohl, B.M.U. Scherzer, Nucl. Instrum. Methods 149 (1978) 59.
[12] J.A. Sawiki, J. Roth, L.M. Howe, J. Nucl. Mater. 162–164 (1989) 1019.
[13] R.S. Blewer, Nucl. Instrum. Methods 149 (1978) 47.
[14] J. L'Ecuyer, C. Brassard, C. Cardinal, J. Chabbal, L. Dechenes, J.P. Labrie, B. Terreault, J.G. Marteland, R. St.-Jaques, J. Appl. Phys. 47 (1976) 381.
[15] B.L. Doyle, P.S. Peery, Appl. Phys. Lett. 34 (1979) 811.
[16] J. Roth, B.M.U. Scherzer, R.S. Blewer, D.K. Brice, S.T. Picraux, W.R. Wampler, J. Nucl. Mater. 93&94 (1980) 601.
[17] U. Kreissig, R. Grötzschel, R. Behrisch, Nucl. Instrum. Methods B85 (1994) 71.
[18] V.M. Prozesky, C.L. Churms, J.V. Pilcher, K.A. Springhorn, R. Behrisch, Nucl. Instrum. Methods B84 (1994) 373.
[19] Ch.W. Magee, P.Ch. Wu, Nucl. Instrum. Methods 149 (1978) 529.
[20] R.G. Wilson, ed., Secondary Ion Mass Spectrometry (Wiley, New York, 1989).
[21] I.S.T. Tsong, G.L. Power, D.W. Hoffmann, Nucl. Instrum. Methods 168 (1980) 399.
[22] W.R. Wampler, B.L. Doyle, Nucl. Instrum. Methods A349 (1994) 473.
[23] D.H.J. Goodall, G.M. McCracken, J.P. Coad, R.A. Causey, G. Sadler, O.N. Jarvis, J. Nucl. Mater. 162–164 (1989) 1059.
[24] A.A. Haas, I.S. Youle, A.B. Antoniazzi, W.T. Shmayda, J. Nucl. Mater. 220–222 (1995) 585.
[25] H.E. Grove, D. Elmore, R. Ferraro, R. Ferraro, Nucl. Instrum. Methods 168 (1980) 425.
[26] R. Middleton, J. Klein, D. Fink, Nucl. Instrum. Methods B47 (1990) 409.
[27] M.L. Roberts, C. Velsko, K.W. Turteltaub, Nucl. Instrum. Methods B92 (1994) 459.
[28] H.E. Gove, P.W. Kubik, P. Sharma, S. Datar, U. Fehn, T.Z. Hossian, J. Koffer, J.P. Lavine, T.S. Lee, D. Elmore, Nucl. Instrum. Methods B52 (1990) 502.
[29] F.D. McDaniel, J.M. Anthony, S.N. Renfrow, Y.D. Kim, S.A. Datar, S. Matteson, Nucl. Instrum. Methods B99 (1995) 537.
[30] M. Friedrich, W. Bürger, D. Henke and S. Turuc, in: Proc. 7th Int. Conf. on Heavy Ion Accelerator Techology, Australia, Nucl. Instrum. Methods A (1996) in press.
[31] H.J. Hofmann, G. Bonani, E. Morenzoni, M. Nessi, M. Suter, W. Wöplfli, Nucl. Instrum. Methods B5 (1984) 254.
[32] O. Gruber, M. Kaufmann, W. Köppendörfer, K. Lackner, J. Neuhauser, M. Blaumoser, K. Ennen, J. Gruber, O. Gruber, O. Jandl, J. Nucl. Mater. 121 (1984) 407.
[33] H. Vernickel, M. Blaumoser, K. Ennen, J. Gruber, O. Gruber, O. Jandl, M. Kaufmann, H. Kollotzek, W. Köppendörfer, H. Kotzlowski, E. Lackner, K. Lackner, J. Neuhauser, J.-M. Noterdame, M. Pillsticker, R. Pöhlchen, H. Preis, K.-G. Rauh, H. Röhr, H. Schneider, W. Schneider, U. Seidel, B. Sombach, B. Streibl, G. Venus, F. Wesner, A. Wieczorek, J. Nucl. Mater. 128&129 (1984) 71.
[34] D.J.W. Mous, A. Gottdang, R. von den Broek, R.G. Haitsma, Nucl. Instrum. Methods B99 (1995) 697.
[35] R. Middleton, D. Juenemann, J. Klein, Nucl. Instrum. Methods B93 (1994) 39.
[36] R. Behrisch, A.P. Martinelli, S. Grigull, R. Grötzschel, U. Kreissig, D. Hildebrandt, W. Schneider, J. Nucl. Mater. 220–222 (1995) 590.
[37] D. Schleussner, D. Rösler, J. Becker, W. Knapp, Ch. Edelmann, C. García-Rosales, P. Franzen, R. Behrisch, J. Vac. Sci. Technol. (1997) to be published.
[38] P. Franzen, R. Behrisch, C. García-Rosales, D. Schleussner, D. Rösler, J. Becker, W. Knapp, Ch. Edelmann, Nucl. Fusion (1997) to be published.
[39] J.H. Billon, 'Emittance calculation and measurements for a sputter-type negative-ion source', University of Wisconsin, private communication.
[40] S. Bosch, Max Planck Institut für Plasmaphysik, D-85748 Garching, private communication and to be published.
[41] H. Verbeek, the ASDEX Team, J. Nucl. Mater. 145–147 (1987) 523.
[42] H.H. Andersen, J.F. Ziegler, Hydrogen Stopping Powers and Ranges in all Elements (Pergamon, Oxford, 1977).
[43] R. Behrisch, M. Mayer, C. García-Rosales, J. Nucl. Mater. 233–237 (1996) 673.
[44] M. Mayer, R. Behrisch, H. Planck, J. Roth, G. Dollinger, C.M. Frey, J. Nucl. Mater. 232 (1996) 67.
[45] Staudenmayer, J. Roth, R. Behrisch, J. Bohdansky, W. Eckstein, P. Staib, S. Matteson, S.K. Erents, J. Nucl. Mater. 84 (1979) 149.
[46] A. Kallenbach, R. Dux, V. Mertens, O. Gruber, G. Haas, M. Kaufmann, W. Poschenrieder, F. Ryter, H. Zohm, M. Alexander, K.H. Behringer, M. Bessenrodt-Weberpals, H.-S. Bosch, K. Büchl, A.R. Field, J.C. Fuchs, O. Gehre, A. Herrmann, S. Hirsch, W. Köppendörfer, K. Lackner, K.F. Mast, G. Neu, J. Neuhauser, S. De Plena Hemoel, G. Raupp, K. Schönmann, A. Stäbler, K.-H. Steuer, O. Vollmer, M. Weinlich, W.P. West, T. Zehetbauer, ASDEX Upgrade Team, Nuclear Fusion 35 (1995) 1231.